52nd IEEE Conference on Decision and Control
December 10-13, 2013. Florence, Italy

Acceleration Enhancement Factor for Damped Systems Subject to the Discrete Proximate Time-Optimal Servomechanism

J. V. Flores[1], N. R. Bedin Neto[1], A. T. Salton[1] and J. M. Gomes da Silva Jr.[2]

Abstract— **This paper presents an extension of the Proximate Time-Optimal Servomechanism (PTOS) to deal with damped systems. The traditionally called acceleration discount factor is replaced with an acceleration enhancement factor that allows the controller to be more aggressive in the presence of friction. The stability of the closed-loop system is assessed by casting the PTOS nonlinearities in a sector-bounded framework, leading to a set of linear matrix inequalities (LMIs) conditions to be satisfied by the controller parameters. Simulation results illustrate the effectiveness of the proposed methodology.**

Index Terms— **Proximate Time-Optimal Servomechanism; Control Saturation; Sector-bounded nonlinearity; Linear Matrix Inequalities (LMI).**

I. Introduction

Many methods have been researched to achieve fast tracking response in automatic control systems. When it comes to the double integrator plant, the theoretical limits on performance have long been known to be given by the Time-Optimal Control (TOC), also known as "bang-bang" control [1]. However, the development of a practical controller that achieved such performance proved itself to be a hard challenge. Along with many switching controllers, the TOC suffers from the undesired effects of chattering [2] and it is notoriously not robust to plant uncertainty and sensor noise. These practical issues led to the search of techniques that could achieve a near time-optimal performance without the undesired effects of chattering.

A seminal work that achieves near time-optimal performance in a practical manner is the so-called Proximate Time-Optimal Servomechanism (PTOS), proposed by [3]. The PTOS structure is based on that of the bang-bang controller, but it solves the chattering problem while maintaining good performance results. The basic idea of the PTOS consists in saturating the controller output only when it is practical to do so, that is, when the system output is far from the reference. Then, as the system approaches the reference point, the control law switches to a linear Proportional-Derivative (PD) controller. Since the switching law is continuous, the chattering phenomenon is eliminated. Nevertheless, due to the switching from a TOC-like controller to a PD controller, the performance attained by the PTOS is somehow conservative, leaving room for further developments. Also, since this controller is based on the "bang-bang" strategy specifically designed for double integrator plants, it is not readily generalized for more complex systems.

A different approach has been given in [4] in what came to be known as Composite Nonlinear Feedback (CNF). This strategy is based on the design of a linear control law that provides small damping ratio for fast rise times, associated with a nonlinear function that gradually adds damping to the system as it approaches the reference point, thus avoiding the overshoot. The CNF controller has been generalized and formalized in [5]. One of the features of the CNF is that it takes the input saturation into account only for the stability analysis, not for the design itself. Consequently, the tunning process is dependent of the step reference amplitude in order to achieve a good performance [6]. This fact may result in a tedious tunning process and in a performance loss for large reference steps. However, since this strategy is not based on the "bang-bang" control law, it may be easily applied to a wide range of systems. Recently an attempt to integrate the PTOS and the CNF for high performance control of double integrator plants was proposed in [7].

It is worth highlighting that other control methods such as sliding mode controllers [8] and model predictive control [9] also achieve high performance and may be applicable to several different systems. Some of these controllers consider the saturation levels in the design process, and others do not, some are switching controllers and others are computationally demanding. But more importantly, they are all general strategies that may applied to a wide range of systems. As a consequence, their performance is inferior to that achieved by the PTOS when controlling the double integrator, since the latter was specifically designed for this plant. In principle, a customized PTOS-like controller designed for each specific plant should achieve a better performance than the above approaches. However, it is not an easy task to extend the PTOS approach developed for double integrator plants to other systems [10].

Another key issue regarding the PTOS controllers is the guarantee of the closed-loop stability since, by construction, it is a saturating nonlinear control law [7]. In particular, the nonlinearity embedded in the saturation function is a sector-bounded one. This suggests that the stability of the closed-loop system can be assessed using the absolute stability framework [2], [11]. In this context, some recent papers in the literature addresses the stability analysis of Lur'e type nonlinear systems with saturating state feedback control laws can be inspiring to develop specific conditions to assess the

*This work was in part supported by Capes and CNPq (Brazil).

[1] J. V. Flores, N. R. Bedin Neto and A. T. Salton are with Group of Automation and Control Systems, Pontifical University of Rio Grande do Sul, Av. Ipiranga, 6681, 90619-900 Porto Alegre - RS. Brazil {aurelio.salton, jeferson.flores}@pucrs.br, nelso.bedin@acad.pucrs.br

[2] J. M. Gomes da Silva Jr. is with the Department of Electrical Engineering, Universidade Ferederal do Rio Grande do Sul, Av. Osvaldo Aranha 103, 90035-190 Porto Alegre-RS, Brazil jmgomes@ece.ufrgs.br

stability for PTOS-based control loops [12], [13], [14].

This paper proposes a straightforward extension to the PTOS controller for damped second order systems. The "bang-bang" switching curve, which is the basis for the PTOS, is distorted in order to make the controller more aggressive and achieve a better performance when applied to systems with considerable levels of friction. New stability results that accommodate both the intrinsic input saturation and the nonlinear control law, will be fundamental in order to provide the necessary theoretical background to justify the implementation of the proposed design. The proposed controller will be adapted to the sector-bounded framework presented in [13] and [14], resulting in a set of LMI conditions to ensure the local stability of the closed-loop system. Since the resulting conditions ensure only local stability, an optimization procedure will be presented aiming to maximize an estimate of the region of attraction for the closed loop system. Simulation results will demonstrate that, compared to its original formulation, the proposed PTOS-like controller provides a better performance when applied to damped systems.

II. Preliminaries

This section will be used to introduce the system under consideration and present a brief discussion on the structure of controllers that approximate the time-optimal performance.

The system under consideration is given by a body of mass M subject to some friction whose dynamics is described by the following differential equation $M\ddot{y} = u - c\dot{y}$, where u and y are the system input and output, respectively, and c is the friction coefficient. The state-space representation of this system is given by,

$$\begin{aligned} \dot{x}_1 &= x_2 \\ \dot{x}_2 &= -ax_2 + b\ \mathrm{sat}(u) \\ y &= x_1 \end{aligned} \tag{1}$$

with $a = c/M$, $b = 1/M$ and $x = [x_1\ x_2]'$ representing the position and velocity of the mass. Furthermore, "sat" is the symmetric saturation function defined as $\mathrm{sat}(u) = \mathrm{sign}(u)\cdot\max\{|u|, \bar{u}\}$ with $\bar{u}$ the saturation level of the control input.

The structure and rationale behind the nonlinear functions that constitute a TOC-based controller will be given in the sequel. Figures 1 and 2 highlight three different stages during point-to-point tracking: first, the controller must saturate during acceleration, second, saturate during deceleration, and then asymptotically track the reference.

Recall that the TOC for a double integrator may be expressed in the following feedback form,

$$u_{toc} = \bar{u}\ \mathrm{sign}(\sqrt{2b\bar{u}|e|} - x_2) \tag{2}$$

$$e: = x_1 - y_r \tag{3}$$

where y_r is the desired reference signal [1]. This control law switches between the saturation levels $\pm\bar{u}$ so that the trajectories converge to and stay on the sliding curve,

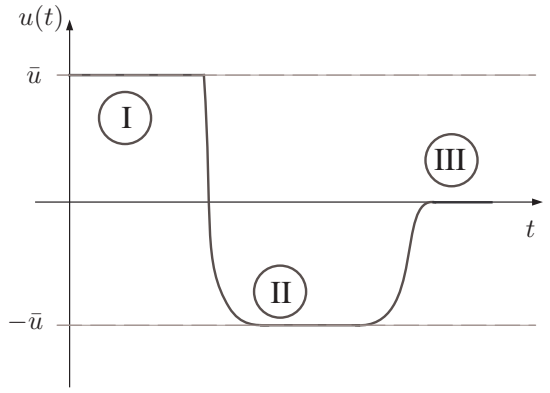

Fig. 1. The three stages of the controller: I maximum acceleration, II smooth transition to maximum deceleration and III asymptotic tracking.

$$x_2 = \sqrt{2b\bar{u}|e|} \tag{4}$$

depicted as the dashed line in Fig. 2 (assuming $\alpha = 1$ in the figure). If the "sign" function is replaced by a gain k_2, i.e.,

$$u = k_2(\mathrm{sign}(e)\sqrt{2b\bar{u}|e|} - x_2), \tag{5}$$

and if k_2 is high enough, the control input will saturate and drive the system towards the sliding curve (stage I). But as soon as x_2 approaches the sliding curve $\sqrt{2b\bar{u}|e|}$, the control signal would approach zero. However, from the theory given by the TOC we know that the control signal should instead switch from upper saturation level to the lower one. This is easily achieved by subtracting the saturation level $\bar{u}$ to equation (5),

$$u = \underbrace{k_2(\mathrm{sign}(e)\sqrt{2b\bar{u}|e|} - x_2)}_{\text{(I)}} - \underbrace{\mathrm{sign}(e)\bar{u}}_{\text{(II)}}.$$

On the above, as (I) goes to zero, the control law is still left with (II), guaranteeing a smooth transition from the positive and negative saturation levels.

Note the above equation may be rearranged to,

$$u = k_2\mathrm{sign}(e)\left(\sqrt{2b\bar{u}|e|} - \frac{\bar{u}}{k_2}\right) - k_2x_2. \tag{6}$$

At this point stages I and II of Figures 1 and 2 are achieved. Notice also that the switching between the saturation levels is smooth and happens approximately at the same time as it does in TOC. However, system (10) under the control signal defined in (6) does not have an equilibrium point at the origin. In fact, it is easy to see that for $x_2 = 0$,

$$|e| = \frac{\bar{u}}{2bk_2^2}.$$

In order to solve the equilibrium point problem and achieve stage III of Fig. 1, the PTOS switches from control law (6) to a linear PD controller guaranteeing asymptotic

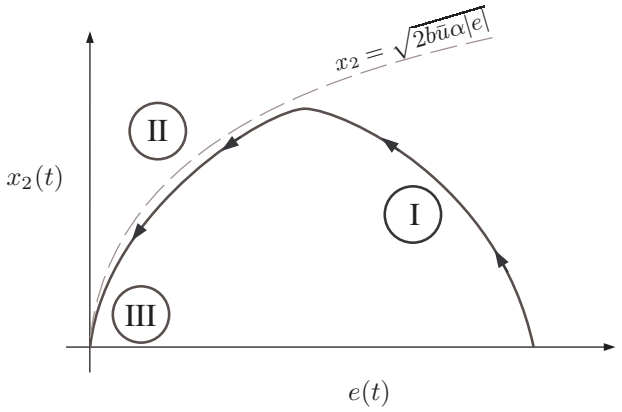

Fig. 2. The three stages of the controller as seen in the e–x_2 phase plane.

tracking and eliminating chattering. The control law becomes,

$$u = k_2(f_{ptos}(e) - x_2), \tag{7}$$

where,

$$f_{ptos}(e) = \begin{cases} (k_1/k_2)e & e \le y_l \\ \text{sign}(e)\left(\sqrt{2b\bar{u}\alpha|e|} - \frac{\bar{u}}{k_2}\right) & e > y_l \end{cases} \tag{8}$$

and $\alpha: \ 0 < \alpha < 1$ is the so called acceleration discount factor, which will be discussed in the sequel. y_l denotes the switching limit between the nonlinear function and the PD controller to be defined in the sequel.

The continuity of the controller is achieved at the boundary $|e| = y_l$ by forcing $f(e^-) = f(e^+)$ and

$$\frac{df(e^-)}{de} = \frac{df(e^+)}{de}.$$

Where $f(e^-)$ and $f(e^+)$ represent the upper and lower lines of (8), respectively. These conditions result in a relation between k_1, k_2 and y_l given by,

$$y_l = \frac{\bar{u}}{k_1}, \quad k_2 = \sqrt{\frac{2k_1}{b\alpha}} \tag{9}$$

III. The Acceleration Enhancement Factor

When applied to double integrator type plants control law (7) presents some undesired overshoot because the PD controller under constraints (9) is not aggressive enough to brake the system in time. Originally, the so called "acceleration discount factor," represented by α in (8), was proposed to solve this problem. The effects of this constant are best understood through Fig. 2 where the TOC switching function is represented by the dashed line for $\alpha = 1$. Obviously, when $\alpha < 1$ the parabola closes towards the error axis, stage I is faster since the trajectories reach the switching curve earlier and the system accelerates for a shorter period of time making it easier for the PD control law to brake the motion before the overshoot happens.

Since the acceleration discount factor adds some conservatism to the solution, creative forms for allowing α to be arbitrarily close to one while avoiding the undesired overshoot have been proposed [7]. Note that $\alpha = 1$ is the time-optimal limit for the double integrator, meaning that above this limit overshoot is unavoidable for these plants because, even if the controller saturates during deceleration, the switching happens too late and the output will pass the reference. In fact, the stability proof presented for the original PTOS relies on the fact that $0 < \alpha < 1$ [15].

When it comes to damped systems, however, this is not necessarily the case. Not only $\alpha = 1$ may be used without overshoot but depending on the friction levels one may desire to allow $\alpha > 1$. This is so because the friction acting on the system will break the symmetry of the trajectories presented in Fig. 2 and it is desirable that the system accelerates for a longer time. In other words, an improved performance may be achieved by prolonging stage I on Figures 1 and 2, which is readily done by choosing $\alpha > 1$. Since this is the scenario of interest in the present paper, henceforth α shall be referred to as the acceleration *enhancement* factor.

Before applying the PTOS strategy with $\alpha > 1$ it is crucial that new stability results are derived. This is carried out in the next section.

IV. Stability Conditions

From a practical perspective, we consider in this paper a discretized implementation of the PTOS controller. In this case, the stability analyis will be carried out considering a discretized version of the plant, obtained by the forward differences method, given by:

$$\begin{aligned} x[k+1] &= Ax[k] + B\text{sat}(u[k]) \\ y[k] &= Cx[k] \end{aligned} \tag{10}$$

with

$$A = \begin{bmatrix} 1 & t_s \\ 0 & 1 - at_s \end{bmatrix}, \ B = \begin{bmatrix} 0 \\ t_s b \end{bmatrix}, \ C = \begin{bmatrix} 1 & 0 \end{bmatrix}$$

where t_s denotes the sampling time.

Due to the special form of $f_{ptos}(e[k])$ the stability of (10) under the PTOS controller can be addressed, without loss of generality, considering $y_r[k] = 0$ and, consequently, $e[k] = x_1[k]$ [7]. Hence, the discretized control signal (7) can be rewritten as

$$u[k] = Kx[k] + \phi_c(L_c x[k]) \tag{11}$$

with $K = \begin{bmatrix} 0 & -k_2 \end{bmatrix}$, $\phi_c(L_c x[k]) = -k_2 f_{ptos}(x_1[k])$ and $L_c = \begin{bmatrix} 1 & 0 \end{bmatrix}$.

From (10) and (11) it follows that the closed-loop system is defined by

$$\begin{aligned} x[k+1] &= (A + BK)x[k] - B\phi(u[k]) + B\phi_c(L_c x[k]) \\ y[k] &= Cx[k] \\ u[k] &= Kx[k] + \phi_c(L_c x[k]) \end{aligned} \tag{12}$$

where

$$\phi(u[k]) = u[k] - \text{sat}(u[k]) \tag{13}$$

is a deadzone nonlinearity. In the sequel, the advantages of considering this deadzone nonlinearity instead of the saturation function will become clear.

In order to apply similar ideas to ones presented in the papers [12], [13] and [14] and to come up with LMI conditions to asses the closed-loop stability, the eigenvalues of $A+BK$ must lie inside the unit circle centered at the origin of the complex plane. Unfortunately, since $K = \left[\begin{array}{cc} 0 & -k_2 \end{array}\right]$ and $B = \left[\begin{array}{cc} 0 & t_s b \end{array}\right]'$, with the controller presented in (11) one of these eigenvalues is always positioned on the unit circle. To overcome this constraint, we consider the addition of an error feedback to the PTOS formulation. In this case, the control law reads

$$u[k] = -k_2 f_{ptos}(e[k]) - k_2 x_2[k] - k_e e[k] \tag{14}$$

which can be written for $y_r = 0$ as

$$u = -k_2 f_{ptos}(x_1[k]) + Fx[k] \tag{15}$$

where

$$F = \left[\begin{array}{cc} -k_e & -k_2 \end{array}\right]. \tag{16}$$

In this formulation, all eigenvalues of $A + BF$ shoud be placed inside the unity disc by an appropriate choice of k_e.

Another fundamental assumption to apply this formulation is to consider the closed-loop system (12) as the feedback connection of a linear system and two sector bounded nonlinearities.

By construction, nonlinearity $\phi_c(e)$ is an odd function that belongs to the sector $(0, \omega_c)$, with $0 < \omega_c < \infty$. This can be clearly seen in Figure 3, which depicts the function ϕ_c for different values of α. In this case, $\phi_c(e) = \phi_c(L_c x)$ globally verifies the following sector condition [1]:

$$\phi_c'(\phi_c - \omega_c L_c x) \leq 0 \tag{17}$$

Also, it has been shown in [16] that the deadzone nonlinearity (13) verifies the so-called "generalized" sector condition give by:

$$\phi'(\phi - Hx - \rho\phi_c) \leq 0 \tag{18}$$

provided that the state belongs to the following region:

$$\mathcal{S} = \left\{ [x' \quad \phi_c]' \in \mathbb{R}^3; |(F-H)x + (1-\rho)\phi_c| \leq \bar{u} \right\}$$

where $H \in \mathbb{R}^{1\times 2}$ and the scalar ρ are free variables to be determined. We are now ready to state stability conditions for the discrete PTOS.

Theorem 1: Consider ω_c and F *a priori* fixed. If there exist a symmetric positive definite matrix $Q \in \mathbb{R}^{2\times 2}$, matrix $X \in \mathbb{R}^{1\times 2}$ and positive scalars ν, θ_c and θ_2 such that the following LMIs are verified

$$\left[\begin{array}{cccc} -Q & * & * & * \\ X & -2\nu & * & * \\ \omega_c L_c Q & \theta_2 & -2\theta_c & * \\ (A+BF)Q & -B\nu & B\theta_c & -Q \end{array}\right] < 0 \tag{19}$$

$$\left[\begin{array}{ccc} Q & * & * \\ -\omega_c L_c Q & 2\theta_c & * \\ FQ - X & \theta_c - \theta_2 & \bar{u}^2 \end{array}\right] > 0 \tag{20}$$

[1]By simplicity, in the developments we denote $\phi(u[k])$ and $\phi_c(e[k])$ as ϕ and ϕ_c respectively

then the trajectories of (12) starting on the ellipsoidal set

$$\mathcal{E}(P,1) = \{x \in \mathbb{R}^2; x'Px \leq 1\}$$

remain bounded to this set and converge asymptotically to the origin.

Proof: Let $V(x) = x[k]'Px[k]$ be a quadratic Lyapunov candidate function and $\Delta V(x) = x[k+1]'Px[k+1] - x[k]'Px[k]$. Assuming $[x'\phi_c]' \in \mathcal{S}$ and that (18) is satisfied globally, if

$$\Delta V(x) - 2\phi_c'\delta_c(\phi_c - \omega_c L_c x) - 2\phi'\kappa(\phi - Hx - \rho\phi_c) < 0 \tag{21}$$

then, $\forall \delta_c, \quad \kappa > 0$, it follows that $\Delta V(x) < 0$. From (12) we have that (21) can be written in the form $\xi'\Lambda\xi < 0$ with $\xi = [x' \ \phi' \ \phi_c']'$ and

$$\Lambda = \left[\begin{array}{ccc} (A+BF)'P(A+BF) - P & * & * \\ -B'P(A+BF) + \kappa H & B'PB - 2\kappa & * \\ B'P(A+BF) + \delta_c\omega_c L_c & -B'PB + \rho\kappa & B'PB - 2\delta_c \end{array}\right].$$

It is important to point out that $\Lambda < 0$ implies that (21) is verified and consequently $\Delta V(x) < 0$. On the other hand, note that Λ can be written in the form

$$\begin{aligned} \Lambda \quad = \quad & \left[\begin{array}{ccc} -P & * & * \\ \kappa H & -2\kappa & * \\ \delta_c\omega_c L_c & \rho\kappa & -2\delta_c \end{array}\right] \\ & + \left[\begin{array}{c} (A+BF)' \\ -B' \\ B' \end{array}\right] P \left[\begin{array}{ccc} (A+BF) & -B & B \end{array}\right] \end{aligned}$$

and, by the Schur complement [17], we have that $\Lambda < 0$ is equivalent to

$$\bar{\Lambda} = \left[\begin{array}{cccc} -P & * & * & * \\ \kappa H & -2\kappa & * & * \\ \delta_c\omega_c L_c & \rho\kappa & -2\delta_c & * \\ A+BF & -B & B & -P^{-1} \end{array}\right] < 0 \tag{22}$$

Consider now $Q = P^{-1}$, $\nu = \kappa^{-1}$, $\theta_c = \delta_c^{-1}$, $X = HQ$ and $\theta_2 = \delta_c^{-1}\rho$. Right and left multiplying (22) by $diag\{Q, \nu, \theta_c, I\}$ it follows that (19) is equivalent to $\bar{\Lambda} < 0$ and therefore we can conclude that (19) implies that (21) is verified. Then, the satisfaction of (19) implies that $\Delta V(x) < -\sigma V(x)$ for some $0 < \sigma < 1$, provided $x[k] \in \mathcal{S}$. This results in $V(x[k+1] < (1-\tau)V(x[k]) = \tau V(x[k])$, with $0 < \tau < 1$. Hence, it follows that $V(x[k]) \leq \tau^{-k}V(x[0])$, $\forall x(0) \in \mathcal{E}(P,1) \subset \mathcal{S}$ which ensures that $\mathcal{E}(P,1)$ is an invariant set and that $x[k] \to 0$ as $k \to \infty$, i.e. that $\mathcal{E}(P,1)$ is included in the region of attraction of the origin of the closed loop system (12).

We show now that relation (20) assures that $\mathcal{E}(P,1) \subset \mathcal{S}$. Note that $\mathcal{E}(P,1) \subset \mathcal{S}$ if

$$\left[\begin{array}{c} x \\ \phi_c \end{array}\right]' \left(\Omega - \left[\begin{array}{c} \bar{F}' \\ \bar{\rho}' \end{array}\right] \frac{1}{\bar{u}} \left[\begin{array}{cc} \bar{F} & \bar{\rho} \end{array}\right]\right) \left[\begin{array}{c} x \\ \phi_c \end{array}\right] \geq 0 \tag{23}$$

$$\forall x, \phi_c \text{ such that } \phi_c'\delta_c(\phi_c - \omega_c L_c x) \leq 0$$

where $\Omega = diag\{P, 0\}$, $\bar{F} = F - G$ and $\bar{\rho} = 1 - \rho$. Applying now the S-procedure and the Schur complement, it follows

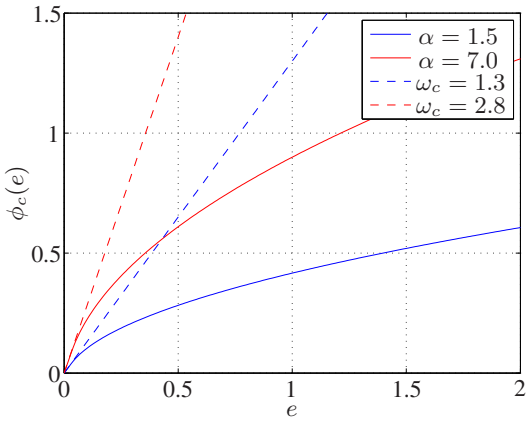

Fig. 3. Nonlinear functions $\phi_c(e)$ and their respective sectors used in the simulations.

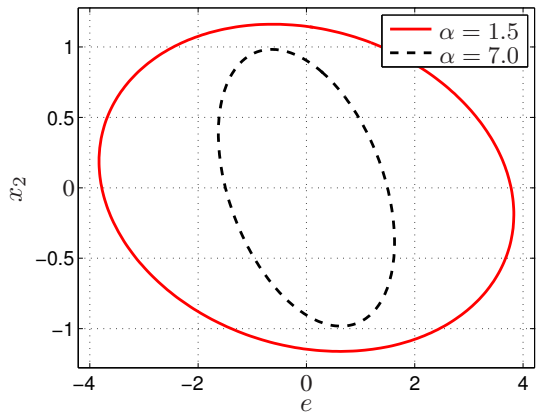

Fig. 4. Ellipsoidal sets $\mathcal{E}(P,1)$ for different values of the acceleration enhancement factor.

that (23) is satisfied if

$$\begin{bmatrix} P & * & * \\ -\delta_c\omega_c L_c & 2\delta_c & * \\ F-H & 1-\rho & \bar{u}^2 \end{bmatrix} > 0 \qquad (24)$$

Finally, pre and post-multiplying (24) by $diag(P, \theta_c, 1)$ it follows that (20) implies (23), which concludes the proof. □

Note that with this approach we can cast the stability proof of the PTOS into the LMI framework, relaxing some conditions in the choice of $f_{ptos}(e[k])$. In particular, α can assume any value provided that ϕ_c belongs to the sector $(0, \omega_c)$ $\forall x \in \mathbb{R}^2$.

Remark 1: An implicit optimization problem is the maximization of $\mathcal{E}(P,1)$ such that conditions in Theorem 1 are satisfied. In [16] are presented the most common size criteria to perform this maximization. In the numerical example to be presented is considered the maximization of the minor axis of $\mathcal{E}(P,1)$ as follows:

$$\max\ \lambda : \begin{cases} Q - \lambda I \geq 0, \\ (19)\text{ - }(20). \end{cases}$$

V. Simulation Results

This section will present a comparison between the proposed design and the traditional PTOS considering the damped model (10). Numerical results were obtained from Matlab R2011b with Yalmip [18] and the solver SeDuMi 1.3 [19].

Let us consider the state-space model (10) with a mass $M = 15$ kg, a friction coefficient of $c = 15$ kg/s, a saturation force of $\bar{u} = 1$ N and a sampling time $t_s = 50$ ms, leading to $a = 1\ \text{s}^{-1}$, $b = 0.07\ \text{kg}^{-1}$. The controller parameters considered in the simulation results are presented in Table I.

TABLE I
PTOS Parameters

α	k_1	k_2	k_e	y_l
1	30	29.2770	0	0.0333
1.5	30	23.9040	1.3790	0.0333
7	30	11.0657	2.8540	0.0333

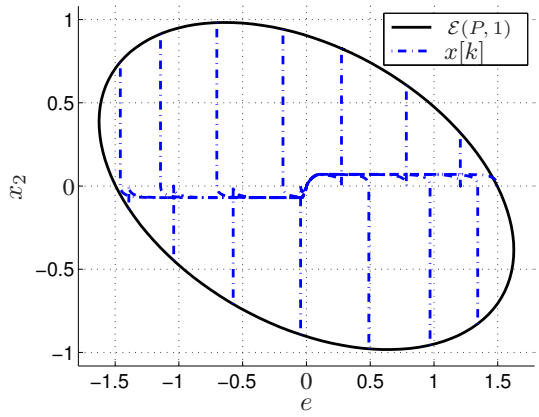

Fig. 5. Trajectories starting at the boundary of $\mathcal{E}(P,1)$ for $\alpha = 7$.

For $\alpha = 1.5$ it follows that the sector-bounded nonlinearity ϕ_c satisfies (17) globally with $\omega_c = 1.3$ and for $\alpha = 7$ this bound results in $\omega_c = 2.8$. In Fig. 3, the plot $\phi_c \times e$ and the corresponding sector bounds given by Ω_c is presented.

Considering the gains in Table I, the solution of the optimization problem from Remark 1 results in

$$P = \begin{bmatrix} 0.0701 & 0.0375 \\ 0.0375 & 0.7612 \end{bmatrix},$$

and $\lambda = 1.3102$ for $\alpha = 1.5$ and

$$P = \begin{bmatrix} 0.4470 & 0.2902 \\ 0.2902 & 1.2239 \end{bmatrix},$$

and $\lambda = 0.7574$ for $\alpha = 7$. The ellipsoidal sets $\mathcal{E}(P,1)$ obtained from matrices P above are presented in Fig. 4. Notice that there is a trade off between the associated stability region and the acceleration enhancement factor. Fig. 5 illustrates the behavior of random trajectories starting on the boundary of $\mathcal{E}(P,1)$ for $\alpha = 7$. It is important to point out that all trajectories converge to the origin as

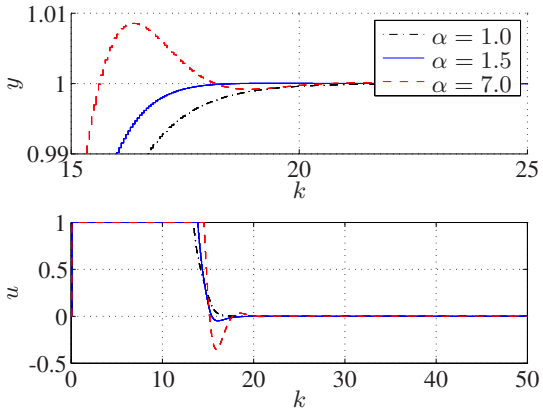

Fig. 6. Unit step response of the comparative controllers. Note that for $\alpha = 7.0$ there is an overshoot of 1%, which may be allowed for performance improvement in some applications.

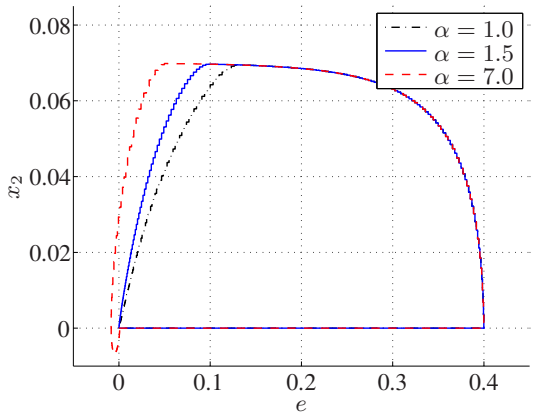

Fig. 7. Phase plane trajectories of the comparative controllers. Note that the higher the acceleration enhancement factor the more aggressive the controller.

$k \to \infty$. Based on this figure we can ensure stability for position excursions over 1.5m long and velocities near to 1.5 m/s. Hence, although our solution is local, the region associated is large enough to satisfy several servomechanism with parameters of similar range to the ones presented in the example.

Fig. 6 shows the response for the 1 m reference. Notice that the acceleration profile of the three controllers is very similar due to the initial saturation. However, controllers with the acceleration enhancement factor remain saturated for a longer period of time, resulting in an improved performance. Also notice that for $\alpha = 7$ the resulting trajectory presents an overshoot smaller than 1%, which might be acceptable in some applications, however, when $\alpha = 1.5$ no overshoot is present. The advantages of the proposed approach are also evidenced in Fig. 7, where the phase plane trajectories for a 0.4 m reference are plotted. As expected, stage I of the controllers using $\alpha > 1$ is longer than that of the original PTOS.

VI. Conclusion

This paper proposed an adaptation of the original PTOS to deal with damped systems. The discrete controller developed here relies on transforming the so called acceleration discount factor into an acceleration enhancement factor. The resulting performance is superior since the system is allowed to accelerate for a longer period of time. Stability conditions of the controller are presented exploring the fact that the nonlinearity in the control law is an odd function and, by definition, belongs to a bounded sector. A set of linear matrix inequalities (LMIs) conditions ensure the local stability of the closed-loop system.

References

[1] E. Arthur, J. Bryson, and Y. Ho, *Applied Optimal Control: Optimization, Estimation, and Control*, ser. Halsted Press book'. Taylor & Francis Group, 1975.

[2] H. K. Khalil, *Nonlinear Systems*, 3rd ed. Prentice Hall, Dec. 2002.

[3] M. L. Workman, R. L. Kosut, and G. F. Franklin, "Adaptive proximate time-optimal servomechanisms: Continuous time case," in *American Control Conference, 1987*, june 1987, pp. 589 –594.

[4] Z. Lin, M. Pachter, and B. S., "Toward improvement of tracking performance-nonlinear feedback for linear systems," *Int. Journal of Control*, vol. 70, pp. 1–11, 1998.

[5] B. Chen, T. Lee, K. Peng, and V. Venkataramanan, "Composite nonlinear feedback control for linear systems with input saturation: theory and an application," *IEEE Transactions on Automatic Control*, vol. 48, no. 3, pp. 427 – 439, mar 2003.

[6] A. Salton, *High Performance Dual-Stage Systems, Control and Design*. Verlag Dr. Mller: Saarbrcken, 2011.

[7] A. Salton, Z. Chen, and M. Fu, "Improved control design methods for proximate time-optimal servomechanisms," *IEEE/ASME Transactions on Mechatronics*, vol. 17, no. 6, pp. 1049 –1058, dec. 2012.

[8] V. I. Utkin, *Sliding Modes in Control and Optimization*. New York: Springer-Verlag, 1992.

[9] G. Goodwin, M. Seron, and J. De Doná, *Constrained control and estimation: an optimisation approach*. Springer, 2004.

[10] L. Pao and G. Franklin, "Proximate time-optimal control of third-order servomechanisms," *IEEE Transactions on Automatic Control*, vol. 38, pp. 560–580, april 1993.

[11] P. Kokotovic and M. Arcak, "Constructive nonlinear control: a historical perspective," *Automatica*, vol. 37, no. 5, pp. 637 – 662, 2001.

[12] E. B. Castelan, U. F. Moreno, J. Corso, and E. R. De Pieri, "Stability and stabilization of a class of uncertain nonlinear discrete-time systems with saturating actuators," in *3rd IFAC Symposium on System, Structure and Control (SSSC)*, 2007, pp. 518–523.

[13] E. B. Castelan, S. Tarbouriech, and I. Queinnec, "Control design for a class of nonlinear continuous-time systems," *Automatica*, vol. 44, no. 8, pp. 2034 – 2039, 2008.

[14] J. M. Gomes da Silva Jr., E. B. Castelan, J. Corso, and D. Eckhard, "Dynamic output feedback stabilization for systems with sector-bounded nonlinearities and saturating actuators," *Journal of the Franklin Institute*, no. 0, pp. –, 2013.

[15] A. M. Pascoal, R. L. Kosut, G. F. Franklin, D. R. Meldrum, and M. L. Workman, "Adaptive time-optimal control of flexible structures," in *American Control Conference, 1989*, june 1989, pp. 19 –24.

[16] S. Tarbouriech, G. Garcia, J. M. Gomes da Silva Jr., and I. Queinnec, *Stability and Stabilization of Linear Systems with Saturating Actuators*. Springer, 2011.

[17] S. Boyd, L. El Ghaoui, E. Feron, and V. Balakrishnan, *Linear Matrix Inequalities in System and Control Theory*, ser. Studies in Applied Mathematics. Philadelphia, PA: SIAM, Jun. 1994, vol. 15.

[18] J. Löfberg, "Yalmip : A toolbox for modeling and optimization in MATLAB," in *Proceedings of the CACSD Conference*, Taipei, Taiwan, 2004. [Online]. Available: http://users.isy.liu.se/johanl/yalmip

[19] J. F. Sturm, "Using sedumi 1.02, a matlab toolbox for optimization over symmetric cones," 1998.